

1 **The Arctic picoeukaryote *Micromonas pusilla* benefits**
2 **synergistically from warming and ocean acidification**

3
4 Clara J. M. Hoppe^{1,2*}, Clara M. Flintrop^{1,3} and Björn Rost¹

5
6 ¹ Marine Biogeosciences, Alfred Wegener Institute – Helmholtz Centre for Polar and Marine
7 Research, 27570 Bremerhaven, Germany

8 ² Norwegian Polar Institute, 9296 Tromsø, Norway

9 ³ MARUM, 28359 Bremen, Germany

10

11 *Correspondence to: Clara J. M. Hoppe (Clara.Hoppe@awi.de)

12

13

14

15 **Abstract**

16 In the Arctic Ocean, climate change effects such as warming and ocean acidification (OA) are
17 manifesting faster than in other regions. Yet, we are lacking a mechanistic understanding of the
18 interactive effects of these drivers on Arctic primary producers. In the current study, one of the
19 most abundant species of the Arctic Ocean, the prasinophyte *Micromonas pusilla*, was exposed
20 to a range of different pCO₂ levels at two temperatures **representing realistic current and future**
21 **scenarios for nutrient-replete conditions**. We observed that warming and OA synergistically
22 increased growth rates at intermediate to high pCO₂ levels. Furthermore, elevated temperatures
23 shifted the pCO₂-optimum of biomass production to higher levels. Based on changes in cellular
24 composition and photophysiology, we hypothesise that the observed synergies can be explained
25 by beneficial effects of warming on carbon fixation in combination with facilitated carbon
26 acquisition under OA. Our findings help to understand the higher abundances of picoeukaryotes
27 such as *M. pusilla* under OA, as has been observed in many mesocosm studies.

28 **1 Introduction**

29 With the progress in using molecular tools to describe marine biodiversity in the past decades,
30 the scientific community has become increasingly aware of the underestimated importance of
31 picoeukaryotes, for both primary and export production of the world's oceans (Richardson and
32 Jackson, 2007; Worden and Not, 2008). Larger phytoplankton such as diatoms are efficient
33 vectors for carbon export due to aggregate formation and ingestion by large zooplankton
34 leading to the production of fast-settling faecal pellets (Sherr et al., 2003). In contrast,
35 picoeukaryotes are mainly grazed by smaller heterotrophic protists such as ciliates, which have
36 a low carbon retention, excrete relatively more dissolved material, and thus fuel recycled
37 production (Sherr and Sherr, 2002). Hence, changes in the relative abundance of pico- and
38 nanoeukaryotes can have large implications for food webs and biogeochemistry (Worden et al.,
39 2015).

40 Picoeukaryotes tend to dominate low nutrient environments, which is often attributed to
41 their high surface:volume ratios and mixotrophic capacities (Raven, 1998; McKie-Krisberg and
42 Sanders, 2014). The low nutrient concentrations in the Arctic surface ocean, for example, cause
43 picoeukaryotes to be particularly successful in this region. In fact, the globally occurring
44 prasinophyte *Micromonas pusilla* is considered the most abundant species in the Arctic ocean
45 (Šlapeta et al., 2006; Lovejoy et al., 2007; Marquardt et al., 2016). In this environment, strong
46 stratification causes **low nutrient concentrations** throughout the summer and autumn months
47 (Tremblay et al., 2015), and the occurrence of the polar night requires organisms to either form
48 resting stages or to have heterotrophic capacities (Tremblay et al., 2009; Lovejoy, 2014; Berge
49 et al., 2015; Vader et al., 2015).

50 Climate change effects manifest faster in the Arctic than anywhere else on the planet
51 (Stocker, 2014). **In this region, for example, temperatures are rising more than twice as fast as**
52 **at the rest of the globe** (Miller et al., 2010). The concurrent rapid reduction in ice cover allows
53 for more light penetration and longer growing seasons, while increased stratification due to ice
54 melt and warming constrain nutrient supply to surface waters, both of which will change the
55 dynamics of primary production (Arrigo et al., 2008; Wassmann and Reigstad, 2011). Ocean
56 acidification (OA) is also especially pronounced in the Arctic Ocean, because low temperatures
57 and alkalinity make the system sensitive to anthropogenic CO₂ loading (AMAP, 2013; Qi et
58 al., 2017). Picoeukaryotes such as *M. pusilla* may benefit from these changes and are considered
59 potential winners of climate change. In the Canadian Arctic, for example, picoeukaryote
60 abundances are increasing as surface waters get warmer, fresher and more oligotrophic (Li et
61 al., 2009). Regarding OA effects, the majority of studies on natural phytoplankton assemblages

62 have shown picoeukaryotes, particularly *M. pusilla*, to increase in relative abundance with
63 increasing pCO₂ levels (Engel et al., 2008; Meakin and Wyman, 2011; Newbold et al., 2012;
64 Brussaard et al., 2013; **Hussherr et al. 2017**; Schulz et al., 2017). Despite the evident sensitivity
65 of *M. pusilla* to changes in pCO₂ levels, a detailed assessment of the OA effects, their
66 interaction with warming as well as the underlying mechanisms in this important species is still
67 missing.

68 Like all photosynthetic organisms, cells of *M. pusilla* need to maintain a balance
69 between energy sources (i.e. light harvesting by the photosynthetic apparatus) and sinks (most
70 importantly carbon fixation in the Calvin cycle) to prevent harmful levels of excitation pressure
71 on the photosynthetic electron transport chain (Behrenfeld et al., 2008). Light harvesting and
72 electron transport in the photosystems are largely independent of changes in temperature and
73 pCO₂ (Mock and Hoch, 2005; Hoppe et al., 2015), but the impact of these drivers on energy
74 sinks can potentially affect the energy balance of the cell: The beneficial effects of elevated
75 pCO₂ observed in phytoplankton are thought to be caused by increased diffusive CO₂ supply,
76 reduced CO₂ leakage, or by lowered costs to operate their CO₂ concentrating mechanisms (Rost
77 et al., 2008; Bach et al., 2013). Elevated temperatures, on the other hand, can change enzyme
78 kinetics including those involved in the Calvin cycle, thus leading to a larger sink of excitation
79 energy (Maxwell et al., 1994; Toseland et al., 2013). Hence, both ocean warming and
80 acidification potentially increase the efficiency of photosynthesis and biomass production, at
81 least up to the organisms' respective optimum levels. Above these levels, temperatures and
82 proton concentrations start to disrupt enzymatic processes, increase **the investment into pH**
83 **homeostasis**, and impair the delicate regulation of cellular processes (Levitt, 1980; Taylor et
84 al., 2001; Flynn et al., 2012). Thus, the complex balance between beneficial and detrimental
85 effects will determine whether the combination of warming and OA will synergistically
86 promote or deteriorate phytoplankton growth and biomass build-up.

87 In the current study, we aim to investigate the responses of an Arctic *M. pusilla* strain
88 to warming and OA. To this end, *M. pusilla* was grown at four pCO₂ levels ranging from
89 preindustrial to future scenarios (180-1400 μatm) under 2°C and 6°C, which represent the
90 magnitude of the projected future temperature increase in this region (Collins et al., 2013), but
91 also the current spring and summer temperatures in the environment where the strain was
92 isolated (Hegseth et al., in press).

93 **2 Material & Methods**

94

95 **2.1 Culture conditions**

96 Monoclonal cultures of the picoeukaryote *Micromonas pusilla* (Butcher) I. Manton & M. Parke
97 (isolated in 2014 by K. Wolf in Kongsfjorden, Svalbard, 79°N; taxonomic identification
98 confirmed by rDNA sequencing of SSU, LSU and ITS sequences) were grown in 1-L glass
99 bottles in semi-continuous dilute-batch cultures (max 129,000 cells mL⁻¹; diluted every 3-4
100 days) under constant irradiances of $150 \pm 26 \mu\text{mol photons m}^{-2} \text{ s}^{-1}$. Media consisted of 0.2 μm
101 sterile-filtered Arctic seawater with a salinity of 32.7 enriched with macronutrients, trace metals
102 and vitamins according to F/2_R medium (Guillard and Ryther, 1962). Light intensities were
103 provided by daylight lamps (Philips Master TL-D 18W; emission peaks at wavelength of 440,
104 560 and 635 nm), adjusted by neutral density screens and monitored using a LI-1400 data logger
105 (Li-Cor) equipped with a 4 π -sensor (Walz). Cells were growing at four different CO₂ partial
106 pressures (pCO₂; 180, 380, 1000, and 1400 μatm) and two temperatures ($2.2 \pm 0.3^\circ\text{C}$ and $6.3 \pm$
107 0.2°C). Cultures were acclimated to these conditions for at least 7 generations prior to sampling.

108 Different pCO₂ conditions were achieved by aeration of the incubation bottles with air
109 of the respective pCO₂ levels delivered through sterile 0.2- μm air-filters (Midisart 2000,
110 Sartorius stedim) for 24 h prior to inoculation. Gas mixtures were generated using a gas flow
111 controller (CGM 2000 MCZ Umwelttechnik), in which CO₂-free air (<1 ppmv CO₂; Dominick
112 Hunter) was mixed with pure CO₂ (Air Liquide Deutschland). The pCO₂ levels in the gas
113 mixtures were regularly monitored with a non-dispersive infrared analyzer system (LI6252, LI-
114 COR Biosciences), calibrated with CO₂-free air and purchased gas mixtures of 150 ± 10 and
115 1000 ± 20 ppmv CO₂ (Air Liquide Deutschland).

116

117 **2.2 Carbonate chemistry**

118 Samples for total alkalinity (A_T) were filtered through 0.7- μm glass fibre filters (GF/F,
119 Whatman) and stored in borosilicate bottles at 3°C. A_T was estimated from duplicate
120 potentiometric titration (Brewer et al., 1986) using a TitroLine alpha plus (Schott Instruments).
121 A_T values were corrected for systematic errors based on measurements of certified reference
122 materials (CRMs provided by Prof. A. Dickson, Scripps, USA; batch #111; reproducibility ± 5
123 $\mu\text{mol kg}^{-1}$). Total dissolved inorganic carbon (C_T) samples were filtered through 0.2- μm
124 cellulose-acetate filters (Sartorius stedim) and stored in gas-tight borosilicate bottles at 3°C. C_T
125 was measured colorimetrically in triplicates with a QuAatro autoanalyzer (Seal; Stoll et al.
126 2001). The analyser was calibrated with NaHCO₃ solutions (with a salinity of 35, achieved by

127 addition of NaCl) to achieve concentrations ranging from 1800 to 2300 $\mu\text{mol C}_T \text{ kg}^{-1}$. CRMs
128 were used for corrections of errors in instrument performance such as baseline drifts
129 (reproducibility $\pm 8 \mu\text{mol kg}^{-1}$). Seawater pH_{total} was measured potentiometrically with a two-
130 point calibrated glass reference electrode (IOLine, Schott Instruments). An internal TRIS-based
131 reference standard (Dickson et al., 2007) was used to correct for variability on electrode
132 performance (reproducibility ± 0.015 pH units). Following recommendations by Hoppe et al.
133 (2012), seawater carbonate chemistry including pCO_2 was calculated from A_T and pH using
134 CO_2SYS (Pierrot et al., 2006). The dissociation constants of carbonic acid of Mehrbach et al.
135 (1973), as refitted by Dickson and Millero (1987), were used for calculations. Dissociation
136 constants for KHSO_4 were taken from Dickson (1990).

137

138 **2.3 Growth, elemental composition and production rates**

139 Samples for cell counts were fixed with glutaraldehyde (0.5% final concentration). After gentle
140 mixing, samples were stored at room temperature in the dark for 15 min, and subsequently
141 frozen in liquid nitrogen and stored at -80°C . Prior to analysis, samples were thawed on ice and
142 mixed thoroughly. After addition of 10 μL SybrGreen working solution (dissolved in DMSO)
143 and 10 μL YG beads working solution (1 μm -Flouresbrite calibration beads grade YG,
144 Polyscience), samples were counted on an Accuri C6 flow cytometer (BD Biosciences)
145 equipped with a blue solid-state laser (488 nm excitation wavelength) run on medium fluidics
146 settings (35 $\mu\text{L min}^{-1}$; 16 μm core size) with a limit of 50,000 events or 250 μL . Analysis was
147 performed based on red (FL3 channel, $>670 \text{ nm}$) and green (FL1 channel, $533 \pm 30 \text{ nm}$)
148 fluorescence, as well as sideward and forward light scattering. Specific growth rates constants
149 (μ) were determined from exponential fits of cell counts over 4 consecutive days.

150 Particulate organic carbon (POC) and nitrogen (PON) were measured after filtration
151 onto precombusted (15h, 500°C) GF/F filters (Whatman) and stored at -20°C . and dried for
152 at least 12 h at 60°C prior to sample preparation. Analysis was performed using a CHNS-O
153 elemental analyser (Euro EA 3000, HEKAtech). Contents of POC and PON were corrected for
154 blank measurements and normalised to filtered volume and cell densities to yield cellular
155 quotas. Production rates of POC were calculated by multiplying the cellular quota with **the**
156 **division rate constant k of the respective incubation**. Samples for determination of chlorophyll
157 a (Chl a) were filtered onto GF/F filters (Whatman), immediately placed into liquid nitrogen
158 and stored at -80°C until analysis. Chl a was subsequently extracted in 8 mL 90% acetone at
159 4°C over night. Chl a concentrations were determined on a fluorometer (TD-700, Turner
160 Designs), using an acidification step (1M HCl) to determine phaeopigments (Knapp et al., 1996).

161

162 2.4 Variable **Chl a** fluorescence

163 Photophysiological characteristics, based on photosystem II (PSII) variable **Chl a** fluorescence,
164 were measured using a fast repetition rate fluorometer (FRRf; FastOcean PTX, Chelsea
165 Technologies) in combination with a FastAct Laboratory system (Chelsea Technologies). The
166 excitation wavelength of the fluorometer's light-emitting diodes (LEDs) was 450 nm, and the
167 applied light intensity was 1.3×10^{22} photons $m^{-2} s^{-1}$. The FRRf was used in single turnover
168 mode, with a saturation phase comprising 100 flashlets on a 2 μs pitch and a relaxation phase
169 comprising 40 flashlets on a 50 μs pitch. Measurements from all replicates (n=3) were
170 conducted in a temperature-controlled chamber ($\pm 0.2^\circ C$) at the respective treatment
171 temperature.

172 After subtraction of a blank value, the minimum (F_0 and F_0' for light-and dark-
173 acclimated measurements, respectively) and maximum **Chl a** fluorescence (F_m , and F_m' for
174 light-and dark-acclimated measurements, respectively) were estimated from iterative
175 algorithms for induction (Kolber et al., 1998) and relaxation phase (Oxborough, 2012) after 15
176 min of dark acclimation, which was sufficient to achieve a dark-acclimated state (data not
177 shown). All fluorescence parameters were calculated by standard equations (Genty et al., 1989;
178 Maxwell and Johnson, 2000). Maximum quantum yields of PSII (apparent PSII photochemical
179 quantum efficiency; F_v/F_m) were calculated as

$$180 \quad F_v/F_m = (F_m - F_0)/F_m \quad (1)$$

181 Fluorescence based photosynthesis-irradiance curves (PI) were conducted at six irradiances (I)
182 between 33 and 672 μmol photons $m^{-2} s^{-1}$, with an acclimation time of 10 min per light step.
183 Electron transfer rate through PSII (**ETR** [$mol e^- (mol RCII)^{-1} s^{-1}$]) for each light step was
184 calculated as:

$$185 \quad \text{ETR} = ((F_m' - F_0')/F_m') * I \quad (2)$$

186 Following the suggestion by Silsbe and Kromkamp (2012), the light-use efficiency (α [$mol e^-$
187 $m^{-2} (mol RCII)^{-1} (mol photons)^{-1}$]) and the maximum electron transfer rates per RCII (ETR_{max}
188 [$mol e^- (mol RCII)^{-1} s^{-1}$]) were estimated by fitting the data to the model by (Webb et al., 1974):

$$189 \quad \text{ETR} = ETR_{max} * [1 - e^{-(\alpha * I)/ETR_{max}}] \quad (3)$$

190 The light saturation index (E_k [μmol photons $m^{-2} s^{-1}$]) was then calculated as ETR_{max}/α .
191 Maximum non-photochemical quenching of **Chl a** fluorescence (NPQ) at irradiances of 672
192 μmol photons $m^{-2} s^{-1}$ (i.e. the highest irradiance step of the PI curve) were calculated using the
193 normalized Stern-Volmer coefficient, also termed NSV, as described in McKew et al. (2013):

194 $(F_q'/F_v')-1 = F_0'/F_v'$ (4)

195 where F_q' is the differences between measured and maximal fluorescence (Suggett et al., 2010).

196 F_0' was measured after each light step (with a duration of 90 s).

197

198 **2.5 Statistics**

199 All data is given as the mean of three biological replicates with \pm one standard deviation. To

200 test for significant differences between the treatments, two-way analyses of variance (ANOVA)

201 with additional normality (Kolmogorov-Smirnov) and Post Hoc (Holm-Sidak) tests were

202 performed. The significance level was set to 0.05. Statistical analyses were performed with the

203 program SigmaPlot (SysStat Software Inc, Version 12.5).

204

205 **3 Results**

206

207 **3.1 Carbonate Chemistry**

208 Regular dilution of cultures with pre-aerated seawater medium kept carbonate chemistry stable
209 over the course of the experiment. More specifically, in each bottle the drift in A_T and C_T
210 compared to initial values was $\leq 3\%$ and $\leq 4\%$, respectively (data not shown). Final carbonate
211 chemistry in the 2°C treatments yielded $p\text{CO}_2$ levels of 197 ± 3 , 323 ± 12 , 959 ± 22 and 1380
212 $\pm 53 \mu\text{atm}$ (Table 1). In the 6°C treatments, $p\text{CO}_2$ levels were 198 ± 6 , 394 ± 10 , 1036 ± 31 and
213 $1449 \pm 18 \mu\text{atm}$. Please note that the same $p\text{CO}_2$ level translates into differing dissolved CO_2
214 concentrations at different temperatures due to the temperature dependency of the carbonate
215 system. Specifically, the treatment $p\text{CO}_2$ values translated into up to 13% lower dissolved CO_2
216 concentrations in the 6°C compared to the 2°C treatment (Table 1; cf. Figure SII).
217 Concurrently, the $p\text{CO}_2$ levels at 2°C corresponded to pH_{total} values of 8.30 ± 0.01 , 8.11 ± 0.01 ,
218 7.68 ± 0.01 and 7.52 ± 0.02 , respectively. In the 6°C treatment, pH_{total} values of the four $p\text{CO}_2$
219 treatments were 8.30 ± 0.01 , 8.04 ± 0.01 , 7.65 ± 0.01 and 7.52 ± 0.01 , respectively.

220

221 **3.2 Growth and biomass build-up**

222 Growth rates constants of exponentially growing *M. pusilla* cultures were significantly affected
223 by the applied treatments (Figure 1, Table 2, SII). Depending on the $p\text{CO}_2$ level, temperature
224 increased growth by 20 to 60% with an average of 0.80 d^{-1} under low and 1.10 d^{-1} under high
225 temperature conditions (two-way ANOVA, $F = 328$, $p < 0.001$). Overall, there was also a
226 positive $p\text{CO}_2$ effect on growth (two-way ANOVA, $F = 9$, $p = 0.001$), even though no linear
227 trends with either $p\text{CO}_2$ or $[\text{CO}_2]$ were observed (Figure 1, SII). The observed $p\text{CO}_2$ responses
228 also differed between temperature levels, indicating a significant interaction between both
229 drivers (two-way ANOVA, $F = 12$, $p < 0.001$): Under low temperature, growth increased
230 significantly from 180 to 380 μatm $p\text{CO}_2$ (post-hoc, $t = 3.1$, $p = 0.04$), while there was a
231 declining, yet insignificant trend in growth with further increases in $p\text{CO}_2$. Under high
232 temperature, growth was significantly higher under 1000 compared to lower (180 μatm ; post-
233 hoc, $t = 5.6$, $p < 0.001$) and higher $p\text{CO}_2$ levels (1400 μatm ; post-hoc, $t = 5.9$, $p < 0.001$). Thus,
234 warming shifted the optimum range for growth to higher $p\text{CO}_2$ levels (Figure 1A).

235 This trend was also observed in terms of POC production rates (Figure 1B, Table 2),
236 with significant effects of temperature (Table SII; two-way ANOVA, $F = 356$, $p < 0.001$), $p\text{CO}_2$
237 (two-way ANOVA, $F = 7$, $p = 0.003$), and their interaction (two-way ANOVA, $F = 29$, p
238 < 0.001). At low temperatures, higher production rates were observed at 180 and 380 μatm

239 compared to those at 1000 and 1400 μatm pCO_2 (post-hoc tests, $t = 3.5$, $p = 0.016$ and $t = 3.0$,
240 $p = 0.046$, respectively). At high temperatures, POC production rates were significantly higher
241 at 1000 μatm than at all other pCO_2 levels (post-hoc tests, e.g. $t = 9.1$, $p < 0.001$ for 380 vs.
242 1000 μatm and $t = 7.4$, $p < 0.001$ for 1000 vs. 1400 μatm), again indicating an upward shift in
243 the pCO_2 optimum with warming.

244

245 **3.3 Cellular composition**

246 Overall, POC quota (Figure 2 a, Table 2, Table SII) were significantly higher under elevated
247 compared to low temperature (two-way ANOVA, $F = 24$, $p < 0.001$), but no overarching trend
248 with pCO_2 was observed. Under low temperature, cells had significantly higher POC quota at
249 low pCO_2 levels (180 and 380 μatm) compared to high pCO_2 levels (1000 and 1400 μatm ; all
250 four post-hoc tests significant, e.g. 380 vs 1000 μatm : $t = 2.8$, $p = 0.033$). This trend reversed
251 under high temperature, where POC quota were highest under 1000 and 1400 μatm (post-hoc
252 test, $t = 3.5$, $p = 0.024$). Thus, temperature and pCO_2 levels exhibited a significant interactive
253 effect on POC quota (two-way ANOVA, $F = 10$, $p < 0.001$).

254 Similar trends were observed in terms of cellular PON quota (Figure 2 b, Table 2, Table
255 SII), where temperature (two-way ANOVA, $F = 5$, $p = 0.045$) and its interaction with pCO_2
256 (two-way ANOVA, $F = 10$, $p < 0.001$) significantly affected the results. Here, opposing pCO_2
257 effects under different temperatures were more subtle, with PON quota under low temperatures
258 only being significantly decreased between 380 and 1400 μatm (post-hoc test, $t = 3.3$, $p =$
259 0.027), while under high temperature PON quota significantly increased from 180 and 380 to
260 1000 μatm pCO_2 (post-hoc tests, $t = 3.7$, $p = 0.012$ and $t = 2.8$, $p = 0.028$, respectively).

261 Regarding cellular Chl *a* quota, there were no significant effects of temperature or pCO_2
262 alone (Figure 2 c, Table 2, Table SII), but a significant interaction between the two drivers
263 (two-way ANOVA, $F = 18$, $p < 0.001$): Under low temperature, Chl *a* quota decreased from low
264 (180 μatm) to high pCO_2 levels (1000 and 1400 μatm ; post-hoc tests, $t = 5.0$, $p < 0.001$ and $t =$
265 3.9 , $p = 0.006$, respectively). Under high temperature, the opposite trend was observed, where
266 Chl *a* quota increased from low (180 and 380 μatm) to high pCO_2 levels (1000 and 1400 μatm ;
267 all four post-hoc tests significant, e.g. 380 vs 1000 μatm : $t = 3.0$, $p = 0.027$).

268 Molar C:N ratios of the biomass (Table 2, Table SII) increased with temperature (two-
269 way ANOVA, $F = 14$, $p = 0.002$), yet this overall difference was mainly driven by results at
270 low pCO_2 levels (180 and 380 μatm ; post-hoc tests, $t = 2.7$, $p = 0.017$ and $t = 3.5$, $p = 0.003$,
271 respectively). By itself, pCO_2 did not significantly affect C:N ratios.

272 The ratios of C:Chl *a* (Figure 2 d, Table 2, Table SII) were elevated under high

273 compared to low temperature conditions (two-way ANOVA, $F = 14$, $p = 0.002$), an effect that
274 was most pronounced at $p\text{CO}_2$ levels of $180 \mu\text{atm}$ (post-hoc test, $t = 5.5$, $p < 0.001$). While there
275 was no effect of $p\text{CO}_2$ on C:Chl *a* at low temperature, C:Chl *a* decreased with increasing $p\text{CO}_2$
276 at high temperature (two-way ANOVA, interaction term, $F = 6$, $p = 0.007$; 180 vs. $1400 \mu\text{atm}$
277 at 6°C post-hoc test, $t = 3.9$, $p = 0.008$).

278

279 **3.4 Chl *a* fluorescence-based photophysiology**

280 The effects of the applied treatments on photophysiology were studied by means of FRRf,
281 which investigates photochemistry at photosystem II (PSII). No effects of the applied
282 treatments were observed in most parameters investigated (Table 3, SI1). This was true for the
283 dark-acclimated quantum yield efficiency of PSII (F_v/F_m), which was similar in all treatments
284 with values of 0.45 ± 0.06 , as well as for absorption cross section of PSII light harvesting (σ_{PSII}).

285 Furthermore, the fitted parameters of FRRf-based PI curves (α , $r\text{ETR}_{\text{max}}$ and E_K) were
286 independent of the experimental treatments (Table 3, SI1). In contrast, the rate constant of the
287 reopening of PSII reaction centres (τ_{ES} ; Table 3, SI1) was slightly yet significantly smaller
288 under high temperatures (two-way ANOVA, $F = 6$, $p = 0.029$), even though this overall
289 response also depended on the applied $p\text{CO}_2$ levels (two-way ANOVA, interaction term, $F = 4$,
290 $p = 0.033$).

291 Maximum non-photochemical quenching (NPQ_{max} ; Table 3, SI1) increased
292 significantly with $p\text{CO}_2$ (Table SI1; two-way ANOVA, $F = 0$, $p = 0.002$) while temperature had
293 no effect. Post-hoc tests revealed that this response was mainly driven by high NPQ_{max} values
294 at $1000 \mu\text{atm}$, which were significantly higher than in any other $p\text{CO}_2$ treatment (e.g. $t = 4.1$, p
295 $= 0.006$ for 380 vs. $1000 \mu\text{atm}$ and $t = 3.1$, $p = 0.030$ for 1000 vs. $1400 \mu\text{atm}$).

296 **4 Discussion**

297

298 **4.1 *Micromonas pusilla* benefits from warming**

299 We observed a strong stimulation of growth rates and biomass build-up with increasing
300 temperature (Figure 1, Table 2). Even though the isolate stems from 1.8°C water temperature,
301 the beneficial effects of warming from 2°C to 6°C are not surprising: *M. pusilla* is known to
302 dominate Arctic phytoplankton assemblages in the summer and autumn situations (Lovejoy et
303 al., 2007; Marquardt et al., 2016) when surface temperatures of 6°C or more can be reached
304 (Hegseth et al., in press). Our results are also in line with mesocosm experiments that indicate
305 stimulatory effects of warming on picoplankton abundances (Daufresne et al., 2009; Sommer
306 et al., 2015) as well as with the temperature optimum of 6-8°C observed for another Arctic
307 strain of *M. pusilla* (Lovejoy et al., 2007).

308 Below the temperature optimum of a cell, warming causes an acceleration of the entire
309 metabolism, as enzymatic reactions run faster under these conditions (Eppley, 1972; Brown et
310 al., 2004). In this study, warming caused higher growth rates, POC quotas and biomass
311 production (Figure 2, Tables 2, SI1), indicating that particularly the fixation and storage of
312 carbon was facilitated by increasing temperature. Electron transport processes, on the other
313 hand, were largely independent of temperature (Tables 3, SI1). Thus, temperature affected the
314 balance between electron transport ('light reaction') and carbon fixation in the Calvin cycle
315 ('dark reactions'). Especially under relatively low temperatures, as investigated here, warming
316 can decrease the excitation pressure on the electron transport chain of the photosystems by
317 increasing the temperature-limited turnover rates of enzyme reaction such as RuBisCO (Mock
318 and Hoch, 2005). Thus, cells grown under low temperature need to invest relatively more
319 energy into biosynthesis than into photochemistry compared to cells grown under high
320 temperature (Toseland et al., 2013). While it has been shown that Antarctic diatoms can
321 compensate for slow RuBisCO kinetics by increasing the expression of this enzyme (Young et
322 al., 2014), it is unknown whether such acclimation responses also occur in prasinophytes.
323 Regarding the C:Chl *a* ratio, this can be taken as an indicator on how much resources the cell
324 retains as carbon biomass (e.g. structural and storage compounds) relative to how much is
325 invested into its light harvesting capacities (Halsey and Jones, 2015). In this study, the strong
326 temperature-dependent increase in C:Chl *a* (Figure 2, Table SI1) under potentially limiting
327 pCO₂ levels of 180 µatm suggests that under warming, the balance between light harvesting
328 and carbon fixation was indeed more beneficial for biomass build-up. Furthermore, elevated
329 temperature significantly decreased τ_{ES} (Table 3, SI1), which can serve as a proxy of the rate

330 at which down-stream processes can remove electrons from PSII (Kolber et al., 1998). Thus,
331 our results indicate that the drainage of electrons into carbon fixation was faster under warmer
332 conditions, explaining the higher growth and biomass production under these conditions.

333

334 **4.2 Warming shifts CO₂ optima towards higher pCO₂ levels**

335 **Under 6°C and pCO₂ levels expected to be reached by the end of this century,** OA had a
336 significantly positive effect on growth and biomass build-up (Figure 1). This finding is in line
337 with previous studies, which have shown that picoeukaryotes can benefit strongly from OA in
338 both laboratory and mesocosm studies (Meakin and Wyman, 2011; Newbold et al., 2012;
339 Schaum et al., 2012; Brussaard et al., 2013; Maat et al., 2014; Schulz et al., 2017). Such positive
340 response to OA could indicate that picoeukaryotes such as *M. pusilla* are mainly dependent on
341 diffusive CO₂ supply and thus directly benefit from higher CO₂ concentrations (Brussaard et
342 al., 2013; Schulz et al., 2013; Schulz et al., 2017).

343 Despite this overall effect, growth rates of *M. pusilla* tended to follow a **non-linear**
344 response curve over the tested range of glacial to elevated future pCO₂ levels (i.e. 180 to 1400
345 µatm), i.e. growth increased with increasing pCO₂ from low to intermediate, but decreased
346 again under the highest pCO₂ levels (Figure 1). Such an optimum behaviour can be expected
347 for most environmental drivers (Harley et al., 2017) and has previously been observed in
348 response to OA (Sett et al., 2014; Wolf et al., 2018). The response patterns in these studies were
349 attributed to a combination of beneficial effects of rising pCO₂ under potentially carbon-
350 limiting conditions for photosynthesis, and negative effects of declining pH on cellular
351 homeostasis and enzyme performance, which manifest mainly at high pCO₂ (Bach et al., 2013).

352 **This non-linearity in the observed pCO₂ effects emphasises the importance of experiments with**
353 **more than two pCO₂ levels in order to properly describe OA-response patterns of organisms.**

354 On a more general level, apparent discrepancies between OA studies can be attributed
355 to actual differences in the environmental settings and their interactive effects with pCO₂
356 (Riebesell and Gattuso, 2015). When comparing the two most commonly applied pCO₂ levels,
357 i.e. the present-day and the anticipated end-of-century situation, the effects of OA on most of
358 the investigated physiological parameters are reversed under 6°C compared to 2°C (Figure 3).
359 This illustrates how difficult it is to infer responses to OA from experiments applying only one
360 set of environmental conditions. It is also noteworthy that the combination of OA and warming
361 led to more densely packed cells (no change in cell size based on flow cytometric
362 measurements; data not shown) with similar stoichiometry compared to the control treatment
363 (Table 2). This indicates that cells managed to cope well with the experienced future conditions.

364 Furthermore, warming altered the OA-dependent change in most of the investigated parameters
365 in a direction that indicates higher fitness compared to low temperatures (e.g. higher growth
366 rates and higher elemental quota; Figure 3). Thus, the increase in growth under future compared
367 to ambient conditions was larger than what would be expected by the respective responses to
368 warming and OA in isolation, indicating synergistic beneficial effects of both drivers.

369

370 **4.3 Potential mechanism underlying the interaction between warming and OA**

371 The observed synergistic effects could be explained by their specific impacts on carbon
372 acquisition and fixation. As outlined in the introduction, light and dark reaction of
373 photosynthesis need to be balanced to achieve high biomass production while avoiding
374 photodamage (Behrenfeld et al., 2008). According to our data, this balance is shifted towards
375 higher biomass production rates under warming and OA.

376 At higher temperatures, seawater CO₂ concentrations were lower than under colder
377 conditions (Table 1; Zeebe and Wolf-Gladrow, 2001). At the same time, warming from 2°C to
378 6°C caused up to 60% higher growth and 110% higher biomass build-up rates (Figure 1, Table
379 2). Furthermore, the decrease in τ_{ES} indicates a faster transfer of photochemical energy into
380 downstream processes such as RuBisCO activity (Table 3). Increased carbon demand in concert
381 with lower carbon supply at higher temperatures thus increases the risk of CO₂ shortage in the
382 cell, which in turn causes OA to have larger effects than at colder temperatures. Moreover,
383 warming changes the kinetics of carbon fixation, with RuBisCO increasing its maximum
384 turnover rates but decreasing its affinity for CO₂ (Young et al., 2014). At higher temperature,
385 cells thus have the potential for higher carboxylation rates provided sufficient CO₂ is available
386 (Kranz et al., 2015). Under elevated pCO₂ levels, diffusive CO₂ supply increases and/or costs
387 for active carbon acquisition decrease. Consequently, the positive effect of increasing
388 temperature on the carbon fixation rate can develop its full potential under OA.

389 In conclusion, elevated catabolic activity under warmer conditions can explain the
390 observed upward shift in the CO₂-optimum of growth with increasing temperature (Figure 1),
391 as the corresponding higher carbon demand causes CO₂ fixation to saturate under higher pCO₂
392 levels. In combination with a faster and more efficient machinery for pH homeostasis at
393 elevated temperatures (Morgan-Kiss et al., 2006), this could explain why declining growth rates
394 were only observed at relatively higher pCO₂ levels compared to those under low temperature
395 conditions (Figure 2).

396 4.4 Implications for the current and future Arctic pelagic ecosystem

397 Picoeukaryotes such as *M. pusilla* are considered to be potential winners of climate change:
398 They are not only thriving in warmer, more stratified environments, which are predicted to
399 further expand in the future, but also seem to benefit from OA (Li et al., 2009; Schulz et al.,
400 2017). Our results for *M. pusilla* confirm beneficial effects of warming and OA on growth and
401 biomass production under nutrient-replete conditions (Figure 1, Table 2). Hence, in warmer
402 spring conditions of the future, this species may experience growth stimulation under OA,
403 potentially increasing its importance early in the growing season. Currently, *M. pusilla* already
404 dominates Arctic phytoplankton assemblages in the nutrient-limited summer and autumn
405 situations, which were not investigated in this study. Regarding the importance of nutrient
406 availability, laboratory experiments found beneficial OA effects on *M. pusilla* primary
407 production to persist also under P limitation (Maat et al., 2014), while in a mesocosm
408 community, OA-dependent increases in *M. pusilla* abundances disappeared when the system
409 ran into P and N co-limitation (Engel et al., 2008). Thus, it remains to be seen how the combined
410 effects of warming and OA manifest under low nutrient conditions as well as how the responses
411 may depend on sources and types of nutrients (e.g. mixing-delivered nitrate vs. regenerated
412 ammonium).

413 A species' success in the environment does not only depend on individual performance, but
414 also on how it compares to that of competing species. When we compare our results with the
415 responses of the Arctic diatom *Thalassiosira hyalina*, isolated from the same location and
416 exposed to the same experimental conditions (Wolf et al., 2018), the diatom had higher growth
417 rates than the picoeukaryote under most treatment conditions, as can be expected for nutrient-
418 replete conditions (Sarhou et al., 2005). The relative increase in growth rates from ambient (2
419 or 3°C and 380 $\mu\text{atm pCO}_2$) to future conditions (6°C and 1000 $\mu\text{atm pCO}_2$) was, however,
420 much higher for *M. pusilla* than for *T. hyalina*. The fact that our experiments were conducted
421 under nutrient-replete conditions, which typically favour diatoms over picoeukaryotes, may
422 indicate an even stronger increase in fitness (Collins et al., 2014) and could mean that *M. pusilla*
423 gains another competitive advantage over phytoplankton like diatoms in the future, in addition
424 to those resulting from changes in stratification (Li et al., 2009). Thus, our findings suggest
425 higher picoplankton contribution to future Arctic phytoplankton assemblages under non-
426 limiting conditions, e.g. early in the growing season when picoeukaryotes can already
427 contribute quite substantially to the phytoplankton standing stocks (Marquardt et al, 2017,
428 Paulsen et al. 2015). How such competition between diatoms and picoeukaryotes would

429 manifest under nutrient-depleted conditions that strongly favour *M. pusilla* is currently
430 unknown.

431 Even though picoeukaryotes seem to contribute more to the downward export of organic
432 matter than previously assumed (Waite et al., 2000; Richardson and Jackson, 2007), in
433 comparison to e.g. diatoms, they are less efficient vectors for carbon export to depth and have
434 a lower energy transfer along trophic levels (Sherr et al., 2003). Consequently, Arctic food webs
435 dominated by picoeukaryotes would look very different from those fuelled by diatom
436 production (Sherr et al., 2003; Paulsen et al., 2015). Due to its motility and capability to grow
437 mixotrophically, *M. pusilla* is characterized by an exceptionally high cellular C:N ratio
438 compared to other Arctic phytoplankton (Table 2; Halsey et al., 2014; McKie-Krisberg and
439 Sanders, 2014). An increased importance of this species would thus not only affect the food
440 web due to its small size and concurrent grazer preferences, but also in terms of food quality
441 (van de Waal and Boersma, 2012). The expected higher growth rates and thus abundances of
442 this species may thus strengthen the Arctic microbial food web. Together with a concurrent
443 weakening of the classical diatom-fuelled food web, this could have severe implications for the
444 flow of energy and nutrients through future marine Arctic ecosystems (Post, 2016).

445

446 **4.5 Conclusions**

447 This study is the first to show synergistic effects of warming and OA on *M. pusilla*, one of the
448 most abundant species of the worlds' oceans. Individually, both warming and OA cause more
449 efficient biomass build-up under nutrient-replete conditions. Beneficial effects manifest,
450 however, even more strongly in combination, when facilitated carbon acquisition (e.g. due to
451 higher diffusive CO₂ supply) co-occurs with higher fixation rates (e.g. due to higher turnover-
452 rates of RuBisCO). Our results provide an explanation for the observations of previous
453 mesocosm studies, which indicated beneficial effects of OA and warming on *M. pusilla* and
454 other picoeukaryotes. Characterising the responses of this Arctic key species to warming and
455 OA will help to develop mechanistic phytoplankton functional types and more realistic model
456 representation of phytoplankton assemblages as well as their responses to multiple drivers.
457 Future studies are needed to elucidate further multifactorial environmental changes, addressing
458 both abiotic (e.g. changes in light and nutrients) as well as biotic (e.g. heterotrophy,
459 competition, grazers, viruses) interactions.

460 **Author Contributions**

461 C.J.M.H. and B.R. designed the study. C.J.M.H. and C.F. conducted the experiment. C.J.M.H.
462 analysed the data and prepared the manuscript with contributions from B.R. and C.F.

463

464 The authors declare that they have no conflict of interest.

465

466

467 **Acknowledgements**

468 We are grateful for field support by the 2014/15 station team of the AWIPEV base in Ny-
469 Ålesund (Svalbard) as well as K. Wolf's help with strain isolation and maintenance of *M.*
470 *pusilla* cultures. We thank U. John and N. Kühne for sequencing and help with the molecular
471 strain identification. Furthermore, L. Wischniewski, A. Terbrüggen and M. Machnik are
472 acknowledged for their help with sample analyses.

References

- AMAP: AMAP Assessment 2013: Arctic Ocean Acidification, Arctic Monitoring and Assessment Programme (AMAP), Oslo, Norway, 99, 2013.
- Arrigo, K. R., van Dijken, G., and Pabi, S.: Impact of a shrinking Arctic ice cover on marine primary production, *Geophysical Research Letters*, 35, L19603, 10.1029/2008gl035028, 2008.
- Bach, L. T., Mackinder, L. C. M., Schulz, K. G., Wheeler, G., Schroeder, D. C., Brownlee, C., and Riebesell, U.: Dissecting the impact of CO₂ and pH on the mechanisms of photosynthesis and calcification in the coccolithophore *Emiliania huxleyi*, *New Phytologist*, n/a-n/a, 10.1111/nph.12225, 2013.
- Behrenfeld, M. J., Halsey, K. H., and Milligan, A. J.: Evolved physiological responses of phytoplankton to their integrated growth environment, *Philosophical Transactions of the Royal Society B: Biological Sciences*, 363, 2687-2703, 10.1098/rstb.2008.0019, 2008.
- Berge, J., Daase, M., Renaud, Paul E., Ambrose, William G., Jr., Darnis, G., Last, Kim S., Leu, E., Cohen, Jonathan H., Johnsen, G., Moline, Mark A., Cottier, F., Varpe, Ø., Shunatova, N., Bałazy, P., Morata, N., Massabuau, J.-C., Falk-Petersen, S., Kosobokova, K., Hoppe, Clara J. M., Węśławski, Jan M., Kukliński, P., Legeżyńska, J., Nikishina, D., Cusa, M., Kędra, M., Włodarska-Kowalczyk, M., Vogedes, D., Camus, L., Tran, D., Michaud, E., Gabrielsen, Tove M., Granovitch, A., Gonchar, A., Krapp, R., and Callesen, Trine A.: Unexpected Levels of Biological Activity during the Polar Night Offer New Perspectives on a Warming Arctic, *Curr. Biol.*, 25, 2555-2561, 10.1016/j.cub.2015.08.024, 2015.
- Brewer, P. G., Bradshaw, A. L., and Williams, R. T.: Measurement of total carbon dioxide and alkalinity in the North Atlantic ocean in 1981, in: *The Changing Carbon Cycle – A Global Analysis* edited by: Trabalka, J. R., and Reichle, D. E., Springer Verlag, Heidelberg Berlin, 358–381, 1986.
- Brown, J. H., Gillooly, J. F., Allen, A. P., Savage, V. M., and West, G. B.: Toward a metabolic theory of ecology, *Ecology*, 85, 1771-1789, 10.1890/03-9000, 2004.
- Brussaard, C. P. D., Noordeloos, A. A. M., Witte, H., Collenteur, M. C. J., Schulz, K., Ludwig, A., and Riebesell, U.: Arctic microbial community dynamics influenced by elevated CO₂ levels, *Biogeosciences*, 10, 719-731, 10.5194/bg-10-719-2013, 2013.
- Collins, M., Knutti, R., Arblaster, J., Dufresne, J.-L., Fichet, T., Friedlingstein, P., Gao, X., Gutowski, W., Johns, T., and Krinner, G.: Long-term climate change: projections, commitments and irreversibility, 2013.
- Collins, S., Rost, B., and Rynearson, T. A.: Evolutionary potential of marine phytoplankton under ocean acidification, *Evolutionary Applications*, 7, 140-155, 10.1111/eva.12120, 2014.

- Daufresne, M., Lengfellner, K., and Sommer, U.: Global warming benefits the small in aquatic ecosystems, *Proceedings of the National Academy of Sciences*, 106, 12788-12793, 10.1073/pnas.0902080106, 2009.
- Dickson, A. G., and Millero, F. J.: A comparison of the equilibrium constants for the dissociation of carbonic acid in seawater media, *Deep-Sea Research*, 34, 1733– 1743, 1987.
- Dickson, A. G.: Standard potential of the reaction: $\text{AgCl(s)} + \frac{1}{2} \text{H}_2(\text{g}) = \text{Ag(s)} + \text{HCl(aq)}$, and the standard acidity constant of the ion HSO_4^- in synthetic seawater from 273.15 to 318.15 K, *Journal of Chemical Thermodynamics*, 22, 113-127, 10.1016/0021-9614(90)90074-Z, 1990.
- Dickson, A. G., Sabine, C. L., and Christian, J. R.: Guide to best practices for ocean CO₂ measurements, North Pacific Marine Science Organization, Sidney, British Columbia, 191, 2007.
- Engel, A., Schulz, K. G., Riebesell, U., Bellerby, R., Delille, B., and Schartau, M.: Effects of CO₂ on particle size distribution and phytoplankton abundance during a mesocosm bloom experiment (PeECE II), *Biogeosciences*, 5, 509-521, 10.5194/bg-5-509-2008, 2008.
- Eppley, R. W.: Temperature and phytoplankton growth in the sea, *Fish. Bull.*, 70, 1063-1085, 1972.
- Flynn, K. J., Blackford, J. C., Baird, M. E., Raven, J. A., Clark, D. R., Beardall, J., Brownlee, C., Fabian, H., and Wheeler, G. L.: Changes in pH at the exterior surface of plankton with ocean acidification, *Nature Clim. Change*, 2, 510-513, 2012.
- Genty, B., Briantais, J.-M., and Baker, N. R.: The relationship between the quantum yield of photosynthetic electron transport and quenching of chlorophyll fluorescence, *Biochimica et Biophysica Acta (BBA) - General Subjects*, 990, 87-92, 10.1016/s0304-4165(89)80016-9, 1989.
- Guillard, R. R. L., and Ryther, J. H.: Studies of marine planktonic diatoms. I. *Cyclotella nana* Hustedt and *Detonula confervacea* Cleve *Can. J. Microbiol.*, 8, 229-239, 1962.
- Halsey, K., Milligan, A., and Behrenfeld, M.: Contrasting Strategies of Photosynthetic Energy Utilization Drive Lifestyle Strategies in Ecologically Important Picoeukaryotes, *Metabolites*, 4, 260-280, 2014.
- Halsey, K. H., and Jones, B. M.: Phytoplankton Strategies for Photosynthetic Energy Allocation, *Annual Review of Marine Science*, 7, null, doi:10.1146/annurev-marine-010814-015813, 2015.
- Harley, C. D. G., Connell, S. D., Doubleday, Z. A., Kelaher, B., Russell, B. D., Sarà, G., and Helmuth, B.: Conceptualizing ecosystem tipping points within a physiological framework, *Ecology and Evolution*, 10.1002/ece3.3164, 2017.
- Hegseth, E. N., Assmy, P., Wiktor, J., Kristiansen, S., Leu, E., Tverberg, V., Gabrielsen, G. W., Skogseth, R., and Cottier, F. R.: Phytoplankton seasonal dynamics in Kongsfjorden,

Svalbard and the adjacent shelf, in: *The Ecosystem of Kongsfjorden, Svalbard*, edited by: Hop, H., and Wiencke, C., Springer, in press.

Hoppe, C. J. M., Langer, G., Rokitta, S. D., Wolf-Gladrow, D. A., and Rost, B.: Implications of observed inconsistencies in carbonate chemistry measurements for ocean acidification studies, *Biogeosciences*, 9, 2401–2405, 10.5194/bg-9-2401-2012, 2012.

Hoppe, C. J. M., Holtz, L.-M., Trimborn, S., and Rost, B.: Ocean acidification decreases the light-use efficiency in an Antarctic diatom under dynamic but not constant light, *New Phytologist*, 207, 159-171, 10.1111/nph.13334, 2015.

Hussherr, R., Levasseur, M., Lizotte, M., Tremblay, J. É., Mol, J., Thomas, H., Gosselin, M., Starr, M., Miller, L. A., Jarníková, T., Schuback, N., and Mucci, A.: Impact of ocean acidification on Arctic phytoplankton blooms and dimethyl sulfide concentration under simulated ice-free and under-ice conditions, *Biogeosciences*, 14, 2407-2427, 10.5194/bg-14-2407-2017, 2017.

Knap, A., Michaels, A., Close, A., Ducklow, H., and Dickson, A.: *Protocols for the Joint Global Ocean Flux Study (JGOFS) Core Measurements.*, UNESCO, 170, 1996.

Kolber, Z. S., Prasil, O., and Falkowski, P. G.: Measurements of variable chlorophyll fluorescence using fast repetition rate techniques. I. Defining methodology and experimental protocols, *Biochem. Biophys. Acta*, 1367, 88-106, 1998.

Kranz, S. A., Young, J. N., Hopkinson, B. M., Goldman, J. A. L., Tortell, P. D., and Morel, F. M. M.: Low temperature reduces the energetic requirement for the CO₂ concentrating mechanism in diatoms, *New Phytologist*, 205, 192-201, 10.1111/nph.12976, 2015.

Levitt, J.: *Responses of Plants to Environmental Stress, Volume 1: Chilling, Freezing, and High Temperature Stresses*, Academic Press., 1980.

Li, W. K. W., McLaughlin, F. A., Lovejoy, C., and Carmack, E. C.: Smallest Algae Thrive As the Arctic Ocean Freshens, *Science*, 326, 539, 10.1126/science.1179798, 2009.

Lovejoy, C., Vincent, W. F., Bonilla, S., Roy, S., Martineau, M.-J., Terrado, R., Potvin, M., Massana, R., and Pedrós-Alió, C.: Distribution, phylogeny, and growth of cold-adapted picoprasinophytes in Arctic Seas, *Journal of Phycology*, 43, 78-89, 10.1111/j.1529-8817.2006.00310.x, 2007.

Lovejoy, C.: Changing Views of Arctic Protists (Marine Microbial Eukaryotes) in a Changing Arctic, *Acta Protozool.*, 53, 91-100, 10.4467/16890027ap.14.009.1446, 2014.

Maat, D. S., Crawford, K. J., Timmermans, K. R., and Brussaard, C. P. D.: Elevated CO₂ and Phosphate Limitation Favor *Micromonas pusilla* through Stimulated Growth and Reduced Viral Impact, *Applied and Environmental Microbiology*, 80, 3119-3127, 10.1128/aem.03639-13, 2014.

- Marquardt, M., Vader, A., Stübner, E. I., Reigstad, M., and Gabrielsen, T. M.: Strong Seasonality of Marine Microbial Eukaryotes in a High-Arctic Fjord (Isfjorden, in West Spitsbergen, Norway), *Applied and Environmental Microbiology*, 82, 1868-1880, 10.1128/aem.03208-15, 2016.
- Maxwell, D. P., Falk, S., Trick, C. G., and Huner, N.: Growth at Low Temperature Mimics High-Light Acclimation in *Chlorella vulgaris*, *Plant Physiology*, 105, 535-543, 10.1104/pp.105.2.535, 1994.
- Maxwell, K., and Johnson, G. N.: Chlorophyll fluorescence—a practical guide, *J. Exp. Bot.*, 51, 659-668, 10.1093/jexbot/51.345.659, 2000.
- McKew, B. A., Davey, P., Finch, S. J., Hopkins, J., Lefebvre, S. C., Metodiev, M. V., Oxborough, K., Raines, C. A., Lawson, T., and Geider, R. J.: The trade-off between the light-harvesting and photoprotective functions of fucoxanthin-chlorophyll proteins dominates light acclimation in *Emiliana huxleyi* (clone CCMP 1516), *New Phytologist*, 200, 74-85, 10.1111/nph.12373, 2013.
- McKie-Krisberg, Z. M., and Sanders, R. W.: Phagotrophy by the picoeukaryotic green alga *Micromonas*: implications for Arctic Oceans, *ISME J*, 8, 1953-1961, 10.1038/ismej.2014.16, 2014.
- Meakin, N. G., and Wyman, M.: Rapid shifts in picoeukaryote community structure in response to ocean acidification, *ISME J*, 5, 1397-1405, 2011.
- Mehrbach, C., Culbertson, C. H., Hawley, J. E., and Pytkowicz, R. M.: Measurement of the apparent dissociation constants of carbonic acid in seawater at atmospheric pressure, *Limnology and Oceanography*, 18, 897-907, 10.4319/lo.1973.18.6.0897, 1973.
- Miller, G. H., Alley, R. B., Brigham-Grette, J., Fitzpatrick, J. J., Polyak, L., Serreze, M. C., and White, J. W. C.: Arctic amplification: can the past constrain the future?, *Quaternary Science Reviews*, 29, 1779-1790, 10.1016/j.quascirev.2010.02.008, 2010.
- Mock, T., and Hoch, N.: Long-Term Temperature Acclimation of Photosynthesis in Steady-State Cultures of the Polar Diatom <i>Fragilariopsis cylindrus</i>, *Photosynth Res*, 85, 307-317, 10.1007/s11120-005-5668-9, 2005.
- Morgan-Kiss, R. M., Priscu, J. C., Pockock, T., Gudynaite-Savitch, L., and Huner, N. P. A.: Adaptation and Acclimation of Photosynthetic Microorganisms to Permanently Cold Environments, *Microbiology and Molecular Biology Reviews*, 70, 222-252, 10.1128/mnbr.70.1.222-252.2006, 2006.
- Newbold, L. K., Oliver, A. E., Booth, T., Tiwari, B., DeSantis, T., Maguire, M., Andersen, G., van der Gast, C. J., and Whiteley, A. S.: The response of marine picoplankton to ocean acidification, *Environmental Microbiology*, 14, 2293-2307, 10.1111/j.1462-2920.2012.02762.x, 2012.

Oxborough, K.: FastPro8 GUI and FRRf3 systems documentation. Chelsea Technologies Group Ltd 2012, 2012.

Paulsen, M. L., Riisgaard, K., Frede, T., St John, M., and Nielsen, T. G.: Winter– spring transition in the subarctic Atlantic: microbial response to deep mixing and pre-bloom production, 2015.

Pierrot, D. E., Lewis, E., and Wallace, D. W. R.: MS Exel Program Developed for CO₂ System Calculations. ORNL/CDIAC-105a Carbon Dioxide Information Analysis Centre, O. R. N. L. (Ed.), US Department of Energy, Oak Ridge, Tennessee, 2006.

Post, E.: Implications of earlier sea ice melt for phenological cascades in arctic marine food webs, *Food Webs*, 10.1016/j.fooweb.2016.11.002, 2016.

Qi, D., Chen, L., Chen, B., Gao, Z., Zhong, W., Feely, R. A., Anderson, L. G., Sun, H., Chen, J., Chen, M., Zhan, L., Zhang, Y., and Cai, W.-J.: Increase in acidifying water in the western Arctic Ocean, *Nature Clim. Change*, 7, 195-199, 10.1038/nclimate3228, 2017.

Raven, J.: The twelfth Tansley Lecture. Small is beautiful: the picophytoplankton, *Funct. Ecol.*, 12, 503-513, 1998.

Richardson, T. L., and Jackson, G. A.: Small Phytoplankton and Carbon Export from the Surface Ocean, *Science*, 315, 838-840, 10.1126/science.1133471, 2007.

Riebesell, U., and Gattuso, J.-P.: Lessons learned from ocean acidification research, *Nature Climate Change*, 5, 12-14, 2015.

Rost, B., Zondervan, I., and Wolf-Gladrow, D.: Sensitivity of phytoplankton to future changes in ocean carbonate chemistry: Current knowledge, contradictions and research needs, *Mar. Ecol. Prog. Ser.*, 373, 227-237, 10.3354/meps07776, 2008.

Sarthou, G., Timmermans, K. R., Blain, S., and Tréguer, P.: Growth physiology and fate of diatoms in the ocean: a review, *J. Sea Res.*, 53, 25-42, 10.1016/j.seares.2004.01.007, 2005.

Schaum, E., Rost, B., Millar, A. J., and Collins, S.: Variation in plastic responses of a globally distributed picoplankton species to ocean acidification, *Nature Climate Change*, 3, 298–302, 10.1038/nclimate1774, 2012.

Schulz, K. G., Bellerby, R. G. J., Brussaard, C. P. D., Bårendsen, J., Czerny, J., Engel, A., Fischer, M., Koch-Klavnsen, S., Krug, S. A., Lischka, S., Ludwig, A., Meyerhöfer, M., Nondal, G., Silyakova, A., Stühr, A., and Riebesell, U.: Temporal biomass dynamics of an Arctic plankton bloom in response to increasing levels of atmospheric carbon dioxide, *Biogeosciences*, 10, 161 - 180, 10.5194/bg-10-161-2013, 2013.

Schulz, K. G., Bach, L. T., Bellerby, R. G. J., Bermúdez, R., Bårendsen, J., Boxhammer, T., Czerny, J., Engel, A., Ludwig, A., Meyerhöfer, M., Larsen, A., Paul, A. J., Sswat, M., and Riebesell, U.: Phytoplankton Blooms at Increasing Levels of Atmospheric Carbon Dioxide:

- Experimental Evidence for Negative Effects on Prymnesiophytes and Positive on Small Picoeukaryotes, *Frontiers in Marine Science*, 4, 10.3389/fmars.2017.00064, 2017.
- Sett, S., Bach, L. T., Schulz, K. G., Koch-Klavsen, S., Lebrato, M., and Riebesell, U.: Temperature Modulates Coccolithophorid Sensitivity of Growth, Photosynthesis and Calcification to Increasing Seawater pCO₂, *PLoS ONE*, 9, e88308, 10.1371/journal.pone.0088308, 2014.
- Sherr, E. B., and Sherr, B. F.: Significance of predation by protists in aquatic microbial food webs, *Antonie Leeuwenhoek*, 81, 293-308, 10.1023/a:1020591307260, 2002.
- Sherr, E. B., Sherr, B. F., Wheeler, P. A., and Thompson, K.: Temporal and spatial variation in stocks of autotrophic and heterotrophic microbes in the upper water column of the central Arctic Ocean, *Deep Sea Research Part I: Oceanographic Research Papers*, 50, 557-571, 10.1016/S0967-0637(03)00031-1, 2003.
- Silsbe, G. M., and Kromkamp, J. C.: Modeling the irradiance dependency of the quantum efficiency of photosynthesis, *Limnol. Oceanogr. Methods*, 10, 645-652, 2012.
- Šlapeta, J., López-García, P. n., and Moreira, D.: Global Dispersal and Ancient Cryptic Species in the Smallest Marine Eukaryotes, *Mol. Biol. Evol.*, 23, 23-29, 10.1093/molbev/msj001, 2006.
- Sommer, U., Paul, C., and Moustaka-Gouni, M.: Warming and ocean acidification effects on phytoplankton—from species shifts to size shifts within species in a mesocosm experiment, *PLoS One*, 10, e0125239, 2015.
- Stocker, T.: *Climate change 2013: the physical science basis: Working Group I contribution to the Fifth assessment report of the Intergovernmental Panel on Climate Change*, Cambridge University Press, 2014.
- Stoll, M. H. C., Bakker, K., Nobbe, G. H., and Haese, R. R.: Continuous-Flow Analysis of Dissolved Inorganic Carbon Content in Seawater, *Analytical Chemistry*, 73, 4111-4116, 2001.
- Suggett, D. J., Borowitzka, M. A., and Prášil, O. E.: *Chlorophyll a Fluorescence in Aquatic Sciences: Methods and Applications*, *Developments in Applied Phycology*, Springer, Dordrecht, 326 pp., 2010.
- Taylor, A. R., Chrachri, A., Wheeler, G., Goddard, H., and Brownlee, C.: A Voltage-Gated H⁺ Channel Underlying pH Homeostasis in Calcifying Coccolithophores, *PLoS Biol.*, 9, 10.1371/journal.pbio.1001085, 2011.
- Toseland, A., Daines, S. J., Clark, J. R., Kirkham, A., Strauss, J., Uhlig, C., Lenton, T. M., Valentin, K., Pearson, G. A., Moulton, V., and Mock, T.: The impact of temperature on marine phytoplankton resource allocation and metabolism, *Nature Clim. Change*, 3, 979-984, 10.1038/nclimate1989, 2013.

- Tremblay, G., Belzile, C., Gosselin, M., Poulin, M., Roy, S., and Tremblay, J. E.: Late summer phytoplankton distribution along a 3500 km transect in Canadian Arctic waters: strong numerical dominance by picoeukaryotes, *Aquat. Microb. Ecol.*, 54, 55-70, 2009.
- Tremblay, J.-É., Anderson, L. G., Matrai, P., Coupel, P., Bélanger, S., Michel, C., and Reigstad, M.: Global and regional drivers of nutrient supply, primary production and CO₂ drawdown in the changing Arctic Ocean, *Progress in Oceanography*, 139, 171-196, 10.1016/j.pocean.2015.08.009, 2015.
- Vader, A., Marquardt, M., Meshram, A. R., and Gabrielsen, T. M.: Key Arctic phototrophs are widespread in the polar night, *Polar Biol*, 38, 13-21, 10.1007/s00300-014-1570-2, 2015.
- van de Waal, D., and Boersma, M.: Ecological stoichiometry in aquatic ecosystems, in: *Encyclopedia of Life Support Systems (EOLSS)*, Developed under the Auspices of the UNESCO (eds. UNESCO-EOLSS Joint Committee), Eolss Publishers, 2012.
- Waite, A. M., Safi, K. A., Hall, J. A., and Nodder, S. D.: Mass sedimentation of picoplankton embedded in organic aggregates, *Limnology and Oceanography*, 45, 87-97, 10.4319/lo.2000.45.1.0087, 2000.
- Wassmann, P., and Reigstad, M.: Future Arctic Ocean seasonal ice zones and implications for pelagic-benthic coupling, *Oceanography*, 24, 220-231, 10.5670/oceanog.2011.74., 2011.
- Webb, W., Newton, M., and Starr, D.: Carbon dioxide exchange of *Alnus rubra*, *Oecologia*, 17, 281-291, 10.1007/bf00345747, 1974.
- Wolf, K., Hoppe, C. J. M., and Rost, B.: Resilience by diversity: Large intraspecific differences in climate change responses of an Arctic diatom, *Limnology and Oceanography*, 63, 397-411, 10.1002/lno.10639, 2018.
- Worden, A. Z., and Not, F.: Ecology and diversity of picoeukaryotes, *Microbial Ecology of the Oceans*, Second Edition, 159-205, 2008.
- Worden, A. Z., Follows, M. J., Giovannoni, S. J., Wilken, S., Zimmerman, A. E., and Keeling, P. J.: Rethinking the marine carbon cycle: Factoring in the multifarious lifestyles of microbes, *Science*, 347, 10.1126/science.1257594, 2015.
- Young, J. N., Goldman, J. A. L., Kranz, S. A., Tortell, P. D., and Morel, F. M. M.: Slow carboxylation of Rubisco constrains the rate of carbon fixation during Antarctic phytoplankton blooms, *New Phytologist*, n/a-n/a, 10.1111/nph.13021, 2014.
- Zeebe, R. E., and Wolf-Gladrow, D. A.: *CO₂ in Seawater: Equilibrium, Kinetics, Isotopes*, Elsevier Science, Amsterdam, 2001.

Table 1: Seawater carbonate chemistry at the end of the experiments (n=3; mean \pm 1 s.d.). CO₂ partial pressure (pCO₂) and dissolved CO₂ concentrations were calculated from total alkalinity (A_T) and pH_{total} at 2 or 6°C, a salinity of 32.7 using CO₂SYS (Pierrot et al., 2006), and phosphate and silicate concentrations of 10 and 100 $\mu\text{mol kg}^{-1}$, respectively. n.a. indicates that values are not available for this specific treatment.

Temperature [°C]	pCO ₂ level [μatm]	pH total scale	A _T [$\mu\text{mol kg}^{-1}$]	C _T [$\mu\text{mol kg}^{-1}$]	dissolved CO ₂ [$\mu\text{mol kg}^{-1}$]	pCO ₂ [μatm]
2	180	8.3 \pm 0.01	2264 \pm 9	2024 \pm 6	11.6 \pm 0.2	197 \pm 3
	380	8.11 \pm 0.01	2244 \pm 30	2124 \pm 11	19.0 \pm 0.7	323 \pm 12
	1000	7.68 \pm 0.01	2255 \pm 45	2215 \pm 23	56.4 \pm 1.3	959 \pm 22
	1400	7.52 \pm 0.02	2243 \pm 5	n.a.	81.1 \pm 3.1	1380 \pm 53
6	180	8.3 \pm 0.01	2243 \pm 28	1969 \pm 10	10.0 \pm 0.3	198 \pm 6
	380	8.04 \pm 0.01	2256 \pm 21	2058 \pm 7	20.0 \pm 0.5	394 \pm 10
	1000	7.65 \pm 0.01	2262 \pm 22	2178 \pm 14	52.6 \pm 1.6	1036 \pm 31
	1400	7.52 \pm 0.01	2265 \pm 5	n.a.	73.6 \pm 0.9	1449 \pm 18

Table 2: Growth rate constants μ , division rate constants k , POC production rates and cellular quota of Chl a , POC and PON as well as their ratios of *M. pusilla* at the end of the experiment under the different treatment conditions (n=3; mean \pm 1 s.d.). Results from statistical analysis can be found in Table SI2.

Temperature [°C]	pCO ₂ [μ atm]	Growth rate constant μ [d ⁻¹]	Division rate constant k [d ⁻¹]	POC production [fmol cell ⁻¹ d ⁻¹]	POC quota [fmol cell ⁻¹]	PON quota [fmol cell ⁻¹]	Chl a quota [fg cell ⁻¹]	POC:PON [mol mol ⁻¹]	POC:Chl a [g g ⁻¹]
2	180	0.75 \pm 0.04	1.08 \pm 0.05	256 \pm 11	239 \pm 20	28.7 \pm 2.6	28.6 \pm 2.1	8.3 \pm 0.1	100 \pm 7
	380	0.85 \pm 0.03	1.23 \pm 0.04	290 \pm 16	237 \pm 22	30.9 \pm 1.8	24.7 \pm 1.4	7.7 \pm 0.3	115 \pm 10
	1000	0.79 \pm 0.05	1.15 \pm 0.07	224 \pm 23	196 \pm 25	24.9 \pm 4.9	20.0 \pm 2.9	8.0 \pm 0.6	118 \pm 5
	1400	0.82 \pm 0.05	1.18 \pm 0.07	235 \pm 13	199 \pm 16	23.9 \pm 2.3	22.0 \pm 1.5	8.4 \pm 0.1	109 \pm 4
6	180	1.06 \pm 0.03	1.53 \pm 0.05	376 \pm 15	245 \pm 3	26.9 \pm 0.6	21.1 \pm 0.8	9.1 \pm 0.1	140 \pm 7
	380	1.05 \pm 0.03	1.52 \pm 0.04	342 \pm 39	226 \pm 26	25.9 \pm 2.5	22.1 \pm 2.6	8.7 \pm 0.3	123 \pm 11
	1000	1.25 \pm 0.05	1.80 \pm 0.07	497 \pm 12	275 \pm 6	33.7 \pm 2.0	27.2 \pm 0.9	8.2 \pm 0.6	122 \pm 6
	1400	1.05 \pm 0.04	1.52 \pm 0.06	400 \pm 14	263 \pm 7	31.1 \pm 1.7	28.6 \pm 3.2	8.5 \pm 0.3	111 \pm 16

Table 3: : FRR-fluorimetric PSII photochemistry measurements – PSII quantum yield efficiency F_v/F_m [dimensionless], functional absorption cross section (σ_{PSII}) [$\text{nm}^{-2} \text{PSII}^{-1}$], rate of PSII re-opening (τ_{ES} [ms]), maximum non-photochemical quenching at 672 $\mu\text{mol photons m}^{-2} \text{s}^{-1}$ (NPQ_{max} [dimensionless]), maximum light-use efficiency (initial slope α [$\text{mol e}^{-} \text{m}^2 (\text{mol RCII})^{-1} (\text{mol photons})^{-1}$]), maximal absolute electron transfer rates through PSII (ETR_{max} [$\text{mol e}^{-} (\text{mol RCII})^{-1} \text{s}^{-1}$]), and the light saturation index (E_K [$\mu\text{mol photons m}^{-2} \text{s}^{-1}$]) under the different temperature and pCO_2 treatments (n=3; mean ± 1 s.d.). Results from statistical analysis can be found in Table SI2.

Temp	pCO_2	F_v/F_m	σ_{PSII}	τ_{ES}	NPQ_{max}	α	ETR_{max}	E_K
2	180	0.50 ± 0.01	8.66 ± 0.35	439 ± 8	2.26 ± 0.18	0.42 ± 0.05	33 ± 2	81 ± 13
	380	0.43 ± 0.09	8.93 ± 0.26	425 ± 4	3.51 ± 0.55	0.32 ± 0.15	25 ± 5	91 ± 44
	1000	0.45 ± 0.08	8.55 ± 0.07	448 ± 1	3.96 ± 0.71	0.42 ± 0.03	31 ± 2	75 ± 10
	1400	0.47 ± 0.10	9.06 ± 0.05	422 ± 14	2.45 ± 0.44	0.43 ± 0.08	31 ± 7	75 ± 31
6	180	0.49 ± 0.01	9.22 ± 0.22	412 ± 6	2.51 ± 0.37	0.49 ± 0.08	28 ± 10	59 ± 28
	380	0.43 ± 0.12	8.83 ± 0.17	427 ± 6	2.83 ± 0.59	0.38 ± 0.09	35 ± 14	90 ± 17
	1000	0.41 ± 0.07	8.91 ± 0.22	422 ± 11	4.94 ± 1.46	0.33 ± 0.09	32 ± 5	100 ± 21
	1400	0.45 ± 0.04	8.71 ± 0.50	428 ± 19	2.93 ± 0.50	0.38 ± 0.04	40 ± 5	104 ± 6

Figure 1: Specific growth rate constant μ (A) and POC production (B) of *M. pusilla* under low (open symbols) and high temperatures (filled symbols) as a function of pCO₂ (n=3; mean \pm 1 s.d.). Results from statistical analysis can be found in Table SI2.

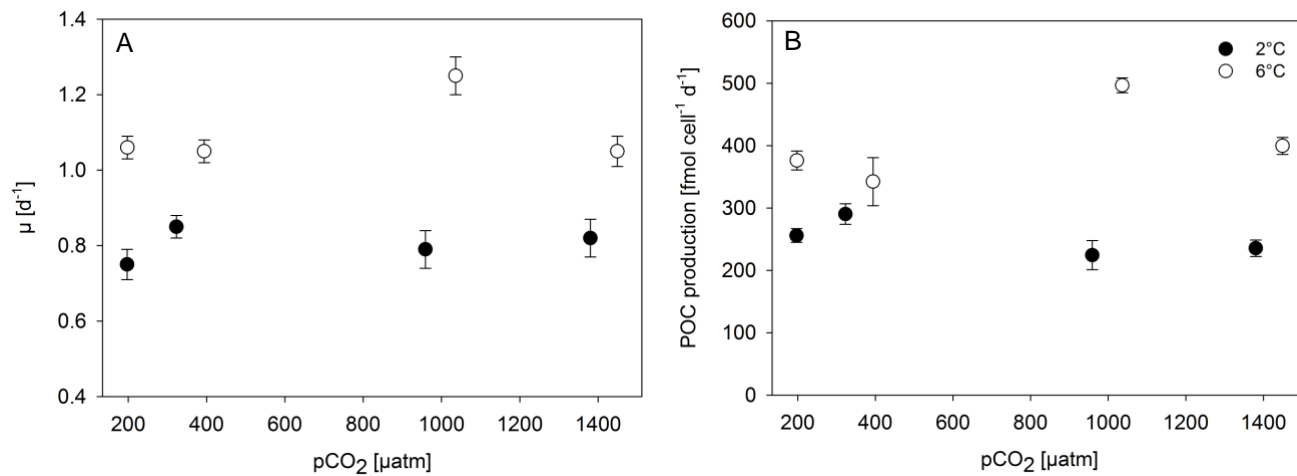


Figure 2: Cellular composition, i.e. POC (A), PON (B) and Chl *a* quota (C) as well as as C:Chl *a* ratios (D), of *M. pusilla* under low (open symbols) and high temperatures (filled symbols) as a function of pCO₂ (n=3; mean ±1 s.d.). Results from statistical analysis can be found in Table SI2.

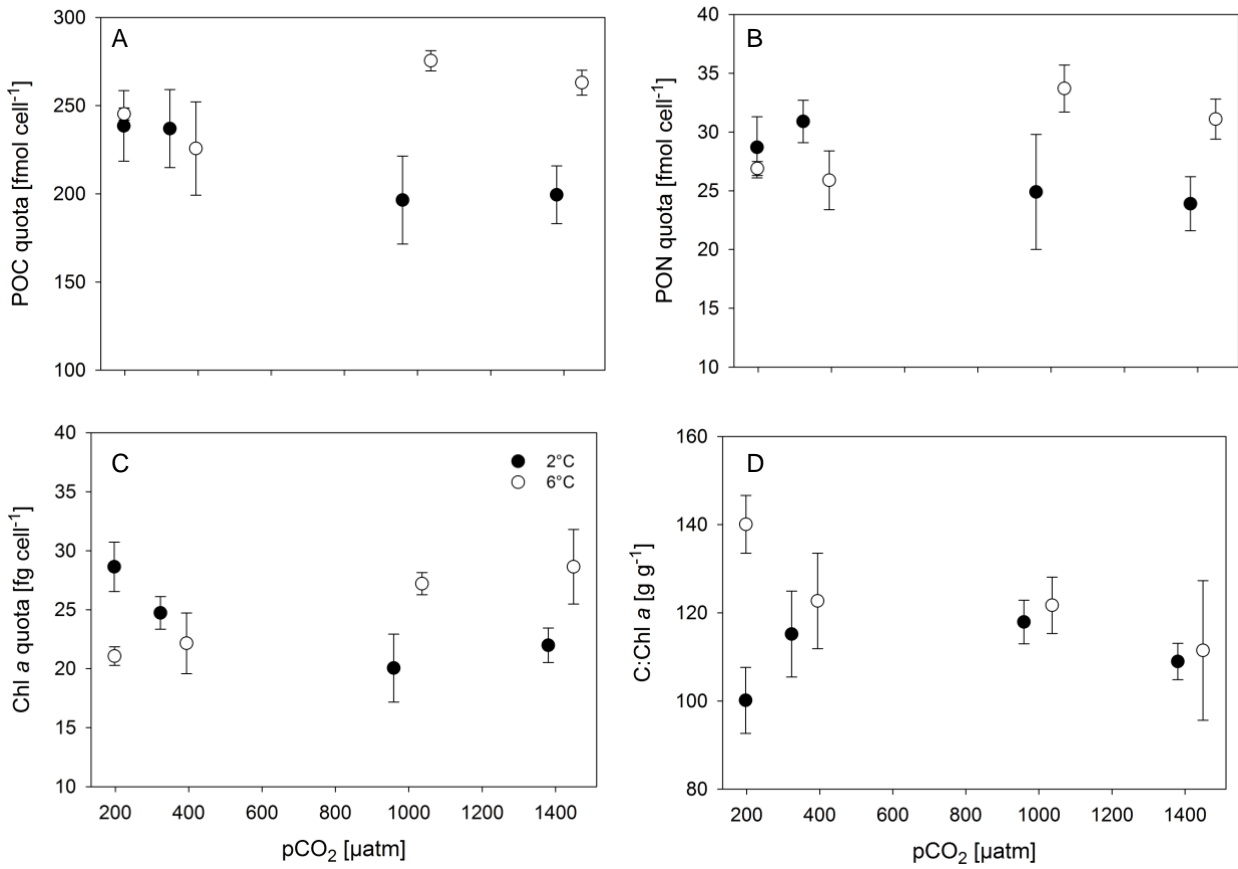
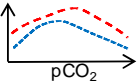
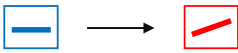
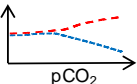
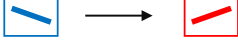
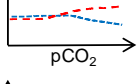
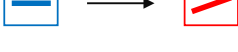
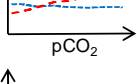

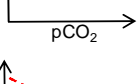



Figure 3: Schematic illustration of results for both temperatures over the entire range of pCO₂ levels as well as focusing on the responses between 380 and 1000 μatm (as the representation for commonly used OA treatments) and their modulation by temperature.

Parameter	Response curves	380 - 1000 μatm effect 2°C → 6°C
Growth		
POC quota		
PON quota		
Chl a quota		
C:N		
C:Chla	